Understanding the interaction between biomacromolecules and their influence on forward osmosis process

Arkhangelsky, Elizabeth; Wicaksana, Filicia; Al-Rabiah, Abdulrahman A.; Al-Zahrani, Saeed M.; Wang, Rong

2016

Arkhangelsky, E., Wicaksana, F., Al-Rabiah, A. A., Al-Zahrani, S. M., & Wang, R. (2016). Understanding the interaction between biomacromolecules and their influence on forward osmosis process. Desalination, 385, 12-23.

https://hdl.handle.net/10356/82755

https://doi.org/10.1016/j.desal.2016.02.006

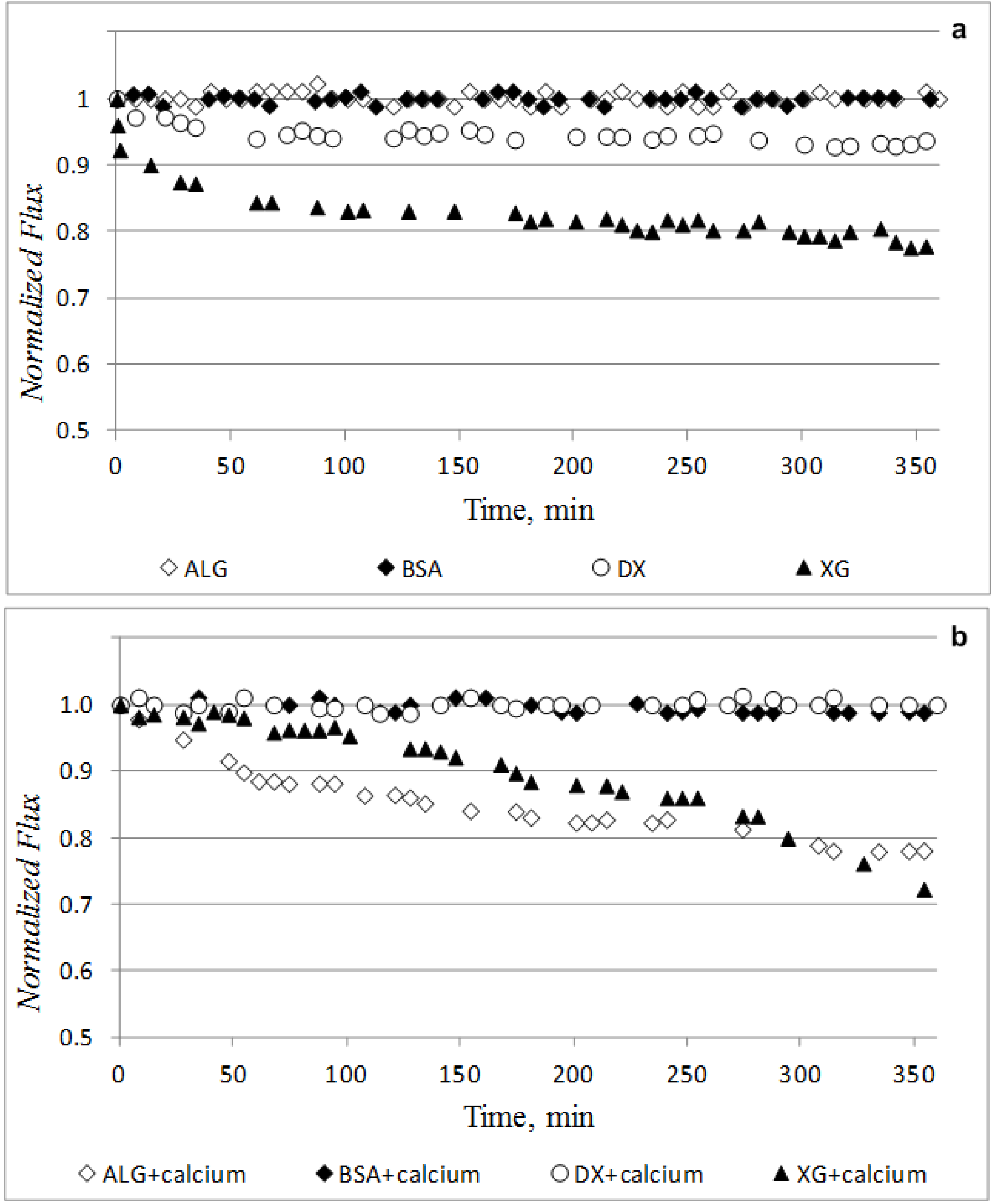

Figure 1. Normalized water flux profiles during filtration of various single foulants. The feed contained 66.7 ppm of foulant and 10 mM NaCl. The concentration of $CaCl_2$ added (Figure 1b) was 1 mM. Experimental conditions: FO mode; cross-flow velocity 6.5 cm/s; draw solution 1 M NaCl; pH 6.25-6.5; temperature 23 °C.

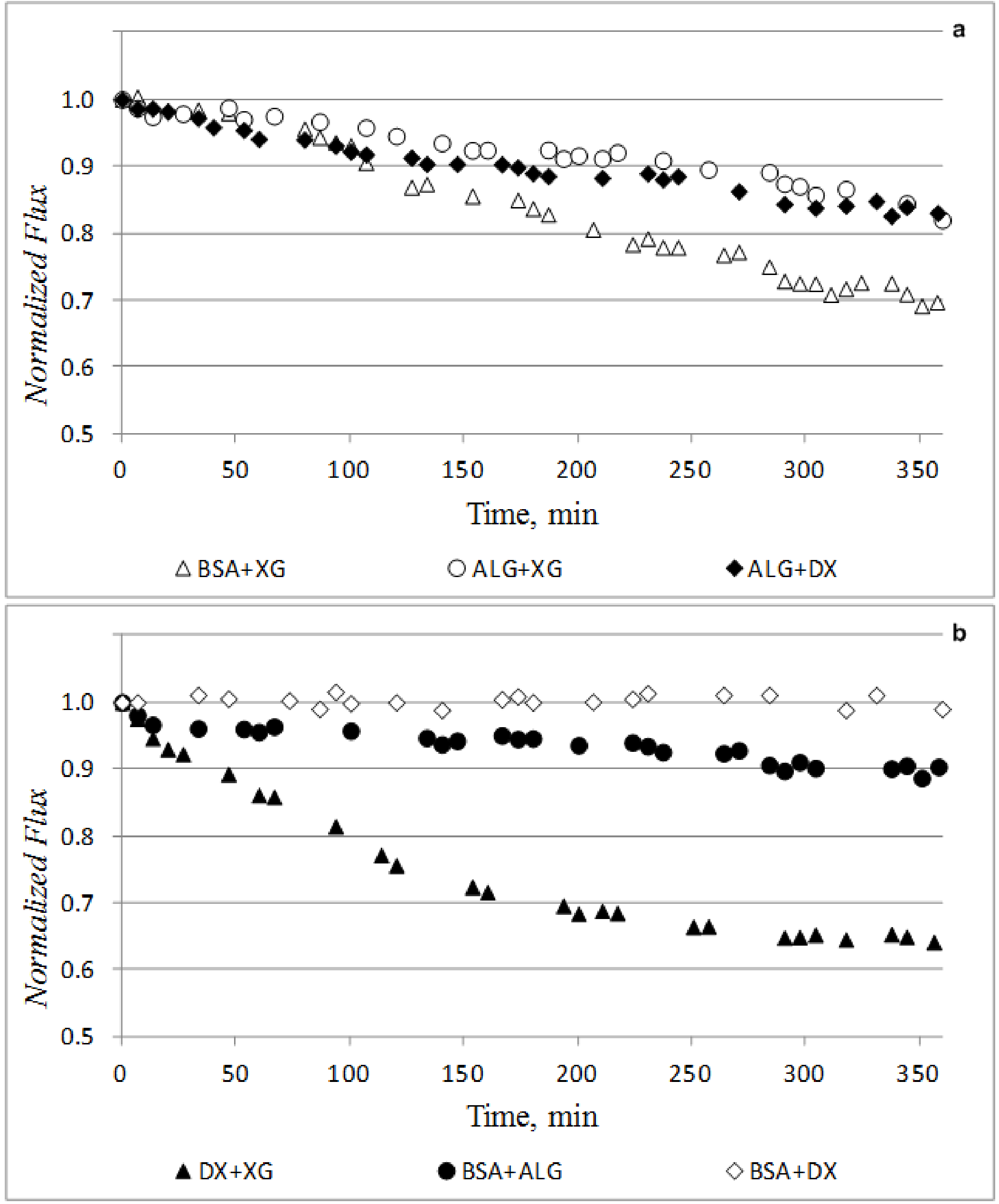

Figure 2. Normalized water flux profiles obtained with various binary foulants. The feed contained 66.7 ppm of each foulant and 10 mM NaCl. Experimental conditions: FO mode; cross-flow velocity 6.5 cm/s; draw solution 1 M NaCl; pH 6.25-6.5; temperature 23 °C.

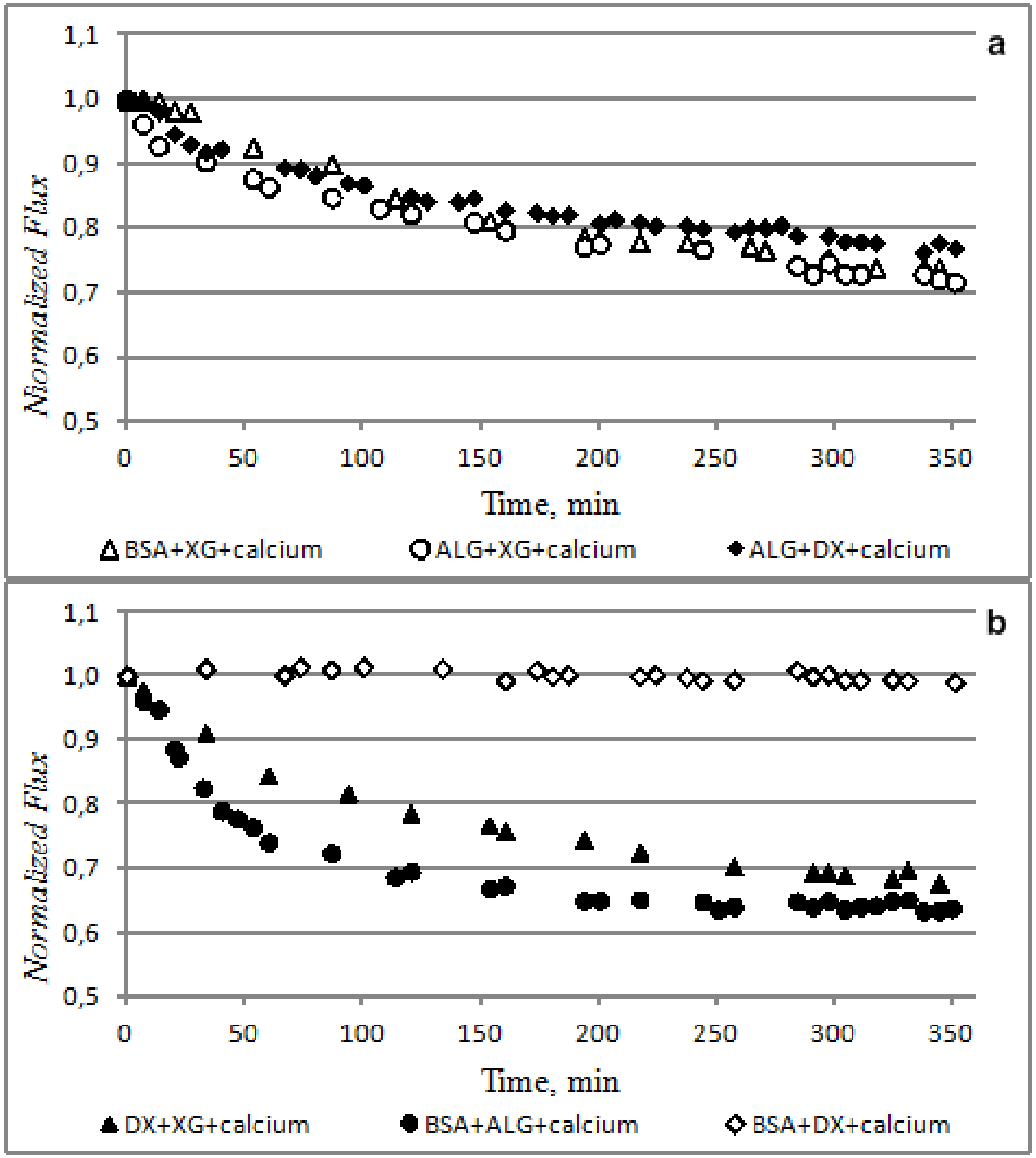

Figure 3. The effect of calcium chloride addition on the performance of FO process with binary foulants. The feed contained 66.7 ppm of each foulant, 10 mM NaCl and 1 mM $CaCl_2$. Experimental conditions: FO mode; cross-flow velocity 6.5 cm/s; draw solution 1 M NaCl; pH 6.25-6.5; temperature 23 °C.

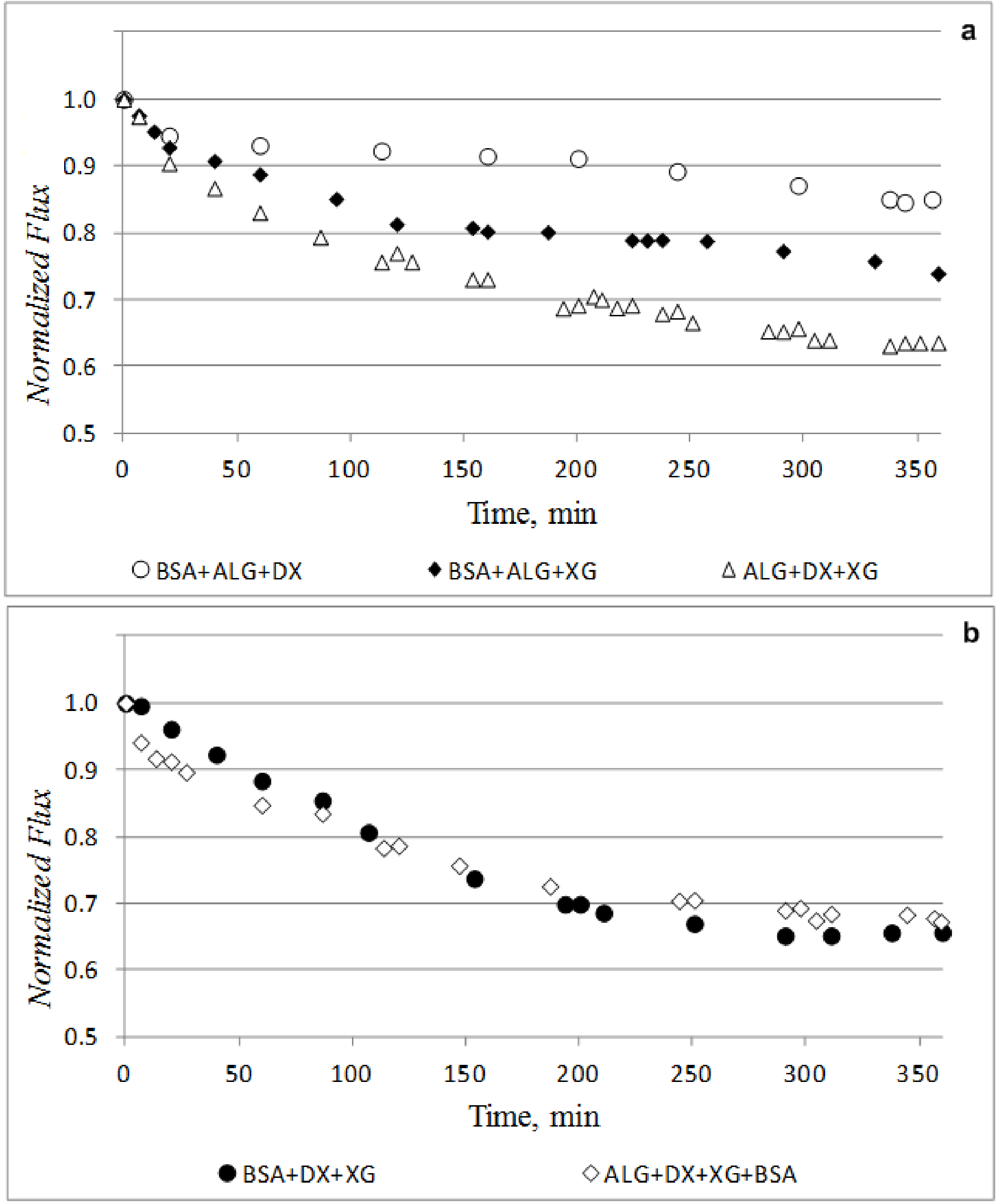

Figure 4. Normalized water flux profiles obtained with ternary and quaternary foulants. The feed contained 66.7 ppm of each foulant and 10 mM NaCl. Experimental conditions: FO mode; cross-flow velocity 6.5 cm/s; draw solution 1 M NaCl; pH 6.25-6.5; temperature 23 °C.

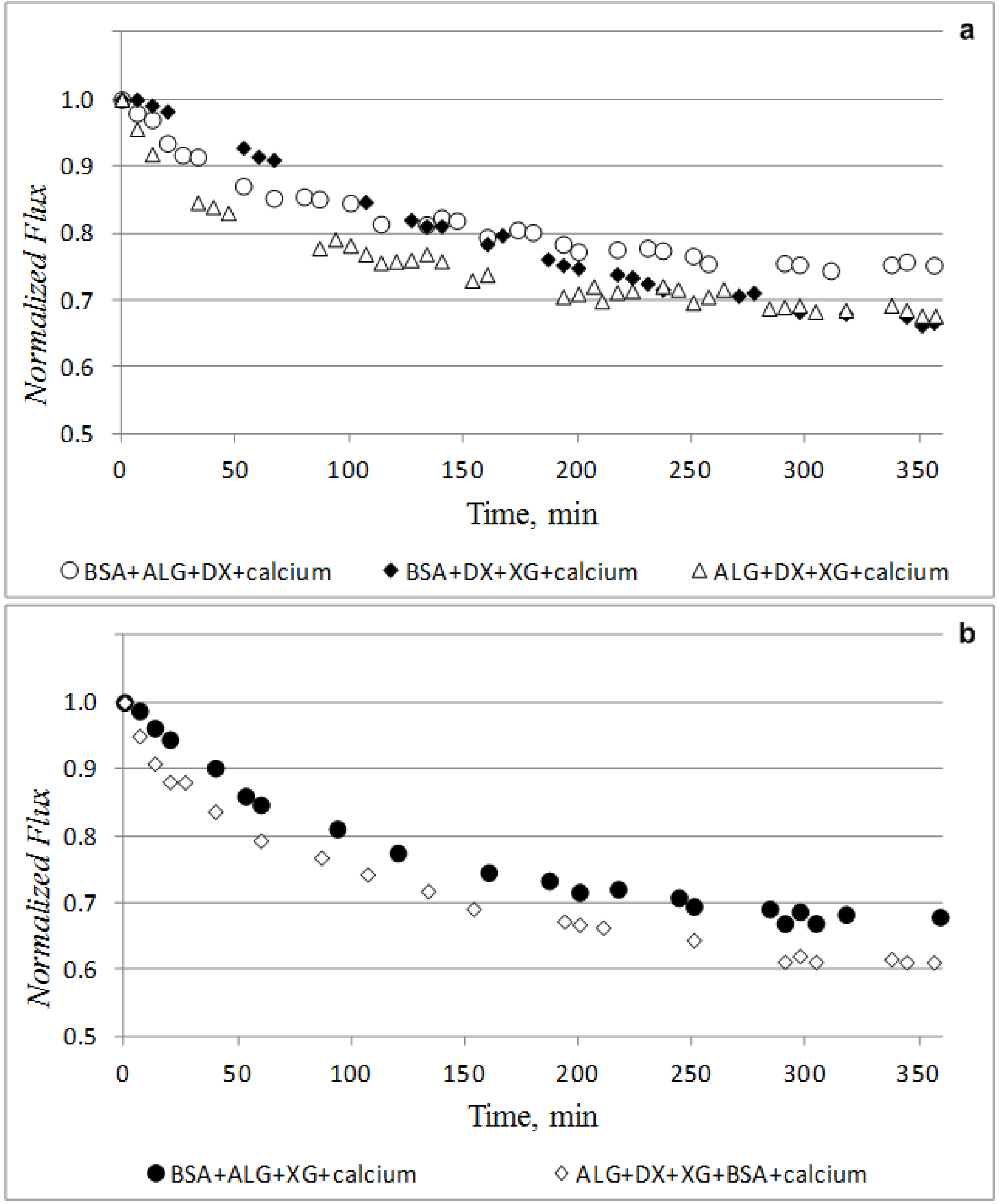

Figure 5. The effect of calcium chloride addition on the performance of FO process with ternary and quaternary foulants. The feed contained 66.7 ppm of each foulant, 10 mM NaCl, 1 mM $CaCl_2$. Experimental conditions: FO mode; cross-flow velocity 6.5 cm/s; draw solution 1 M NaCl; pH 6.25-6.5; temperature 23 °C.

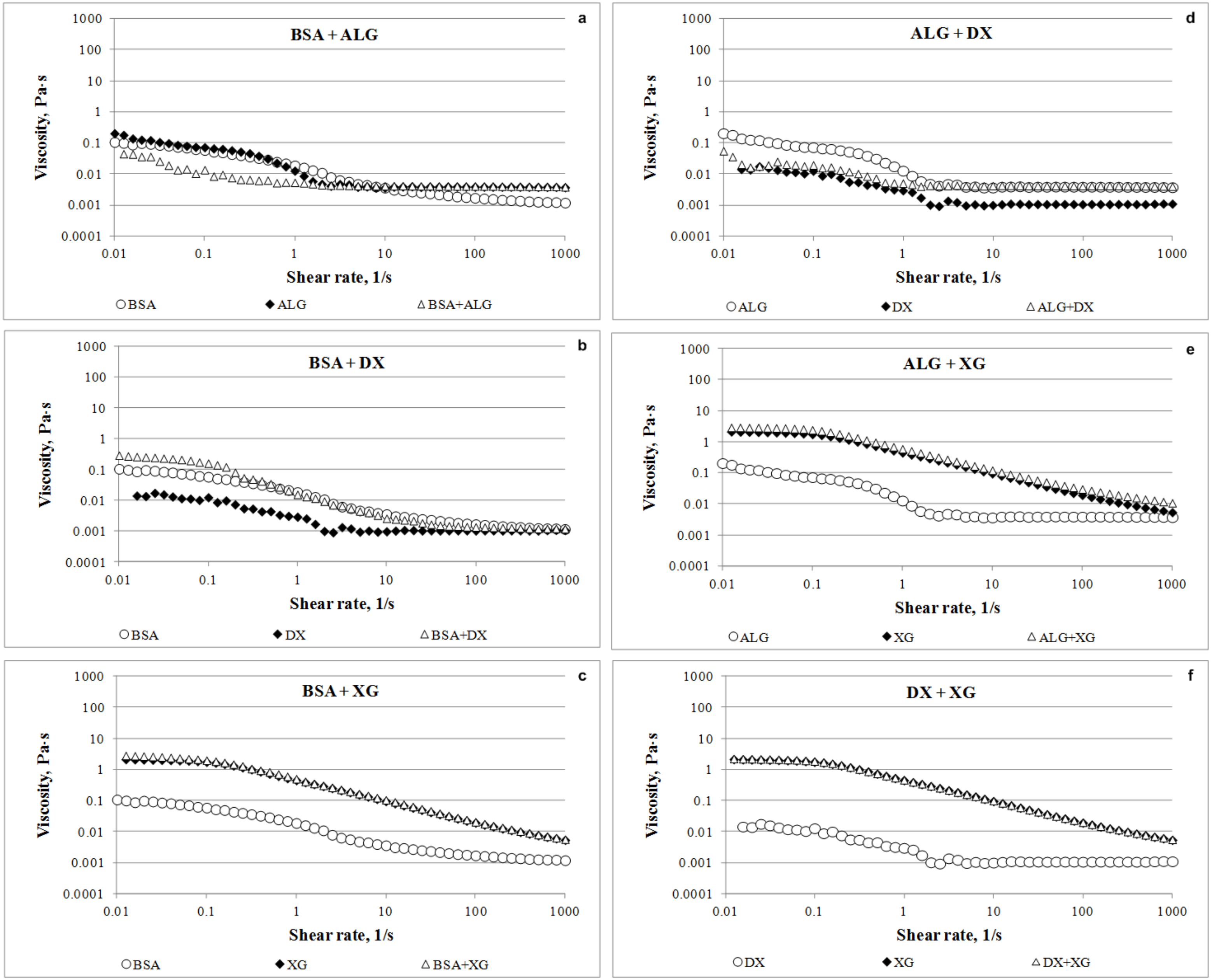

Figure 6. Viscosity of single and binary foulants as a function of shear rate.

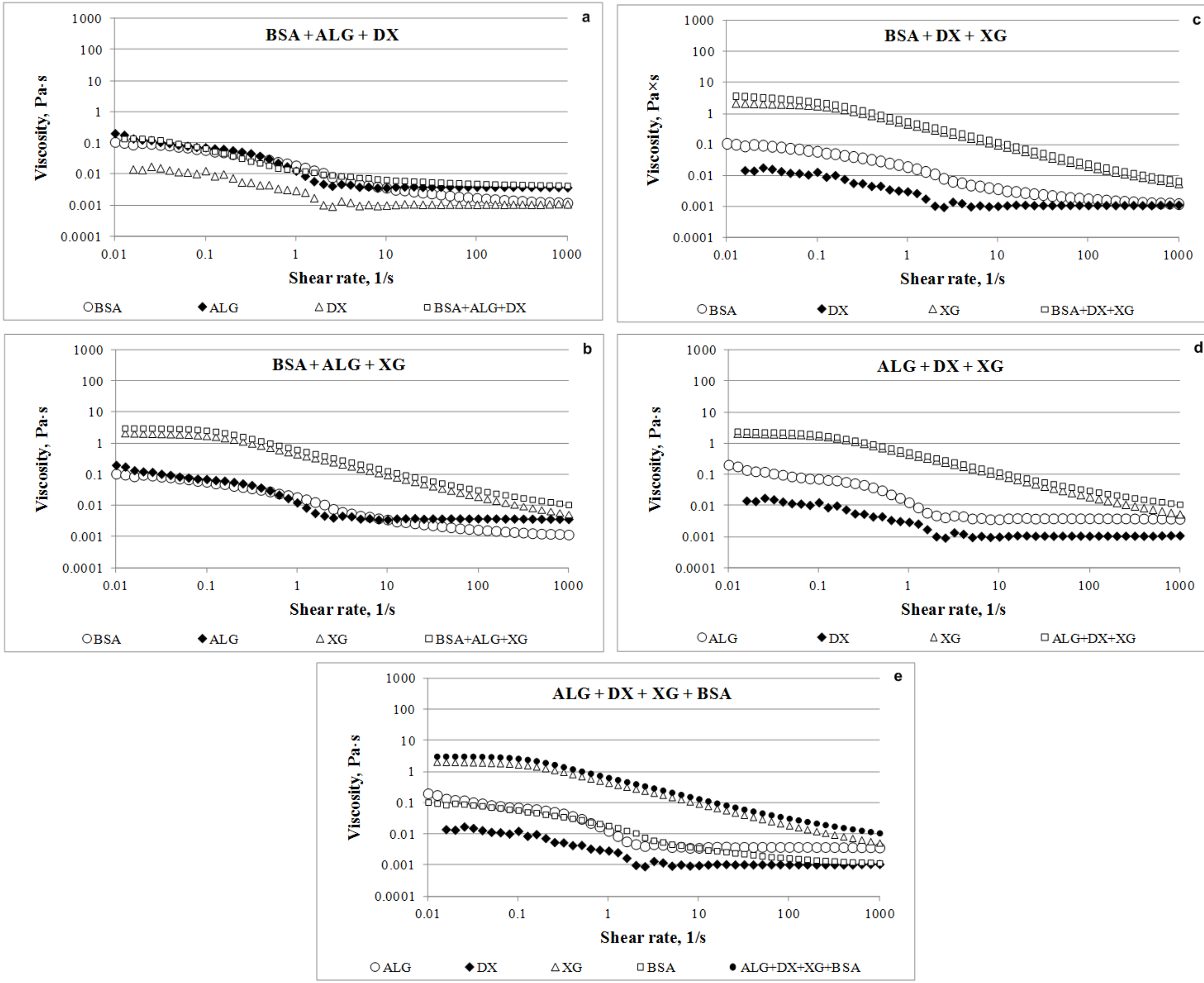

Figure 7. Viscosity of ternary and quaternary foulants as a function of shear rate.

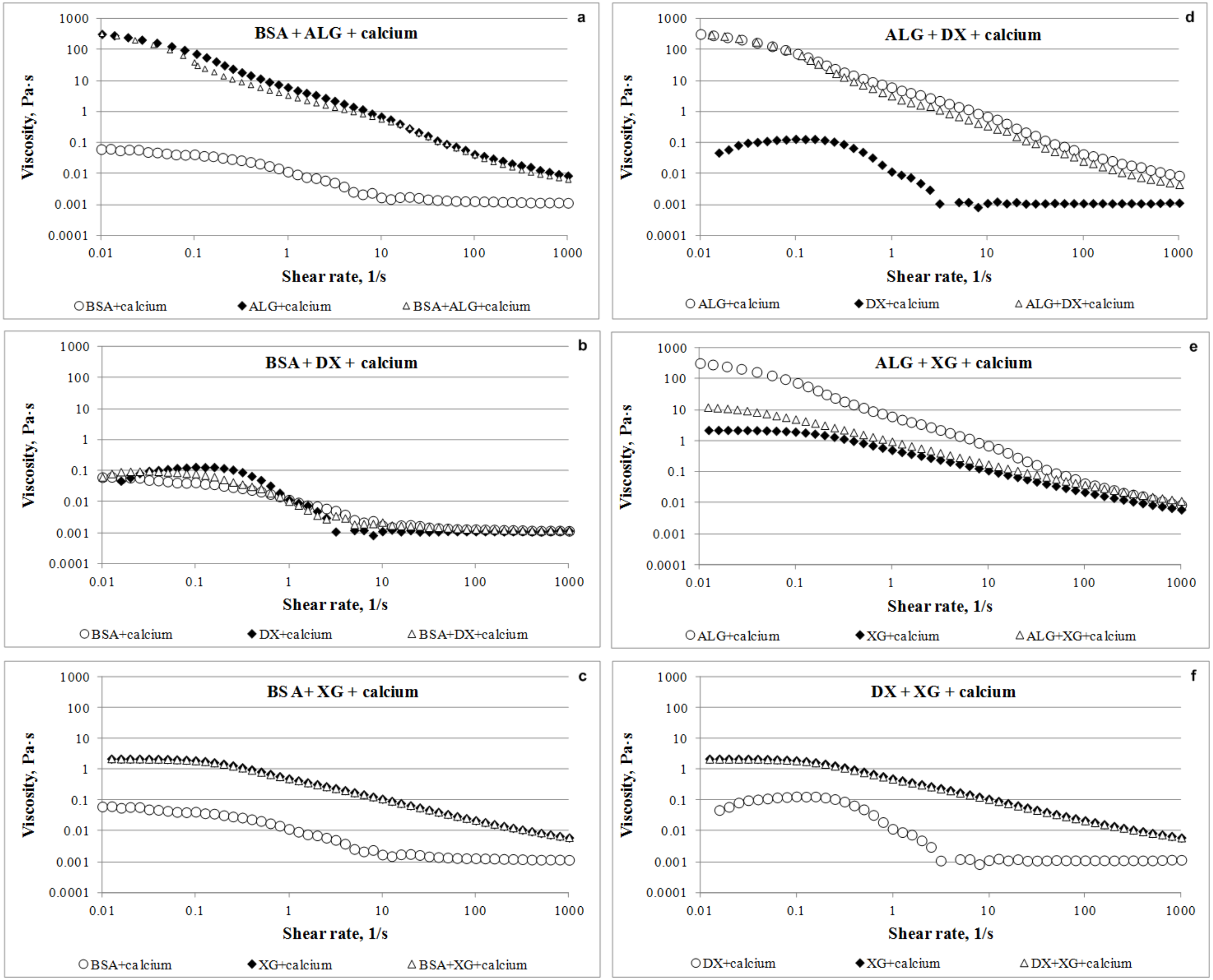

Figure 8. Effect of calcium chloride on viscosity of single and binary foulants within 0.01-1000 s^{-1} shear rate range.

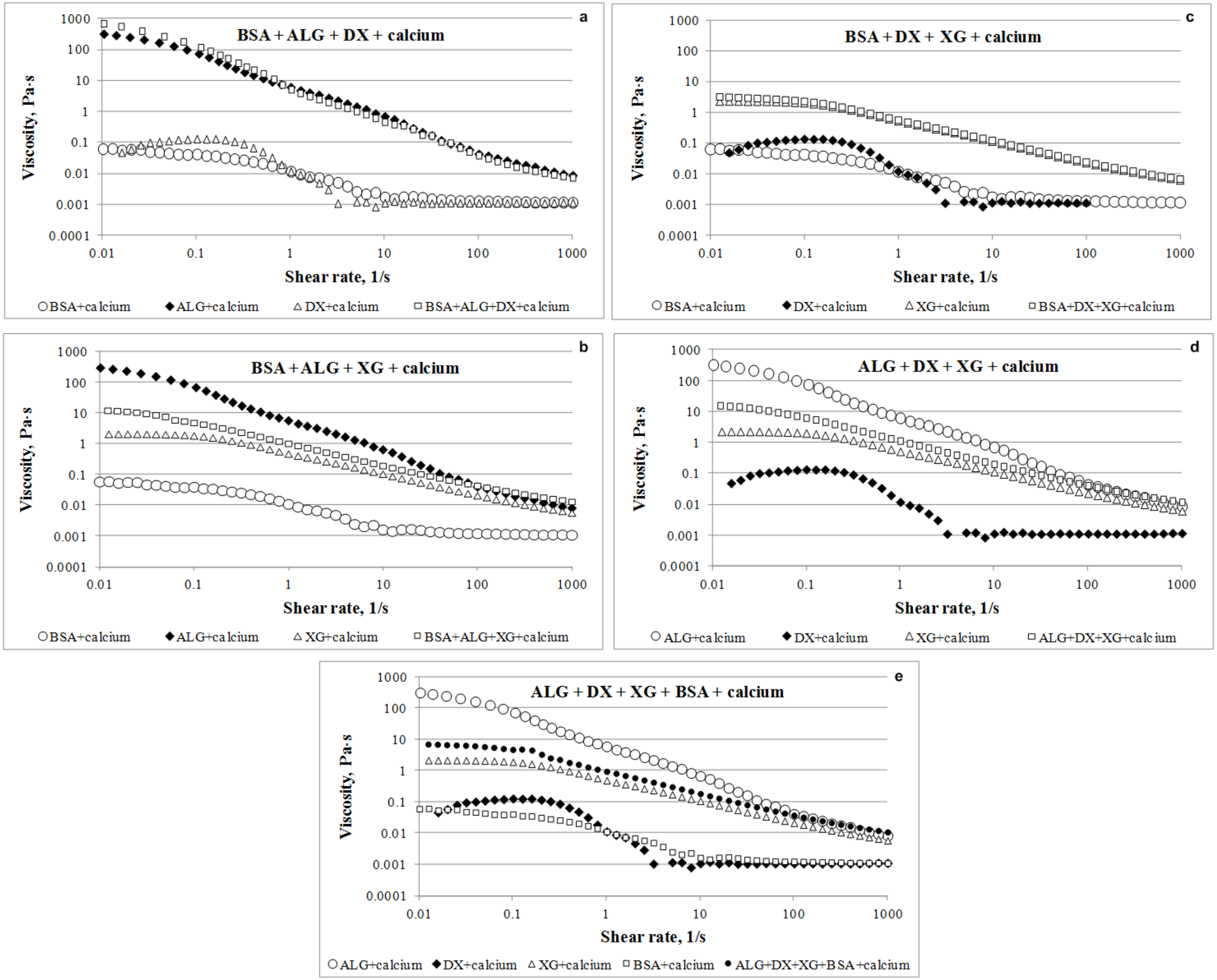

Figure 9. Effect of calcium chloride on viscosity of ternary and quaternary foulants within 0.01-1000 s^{-1} shear rate range.

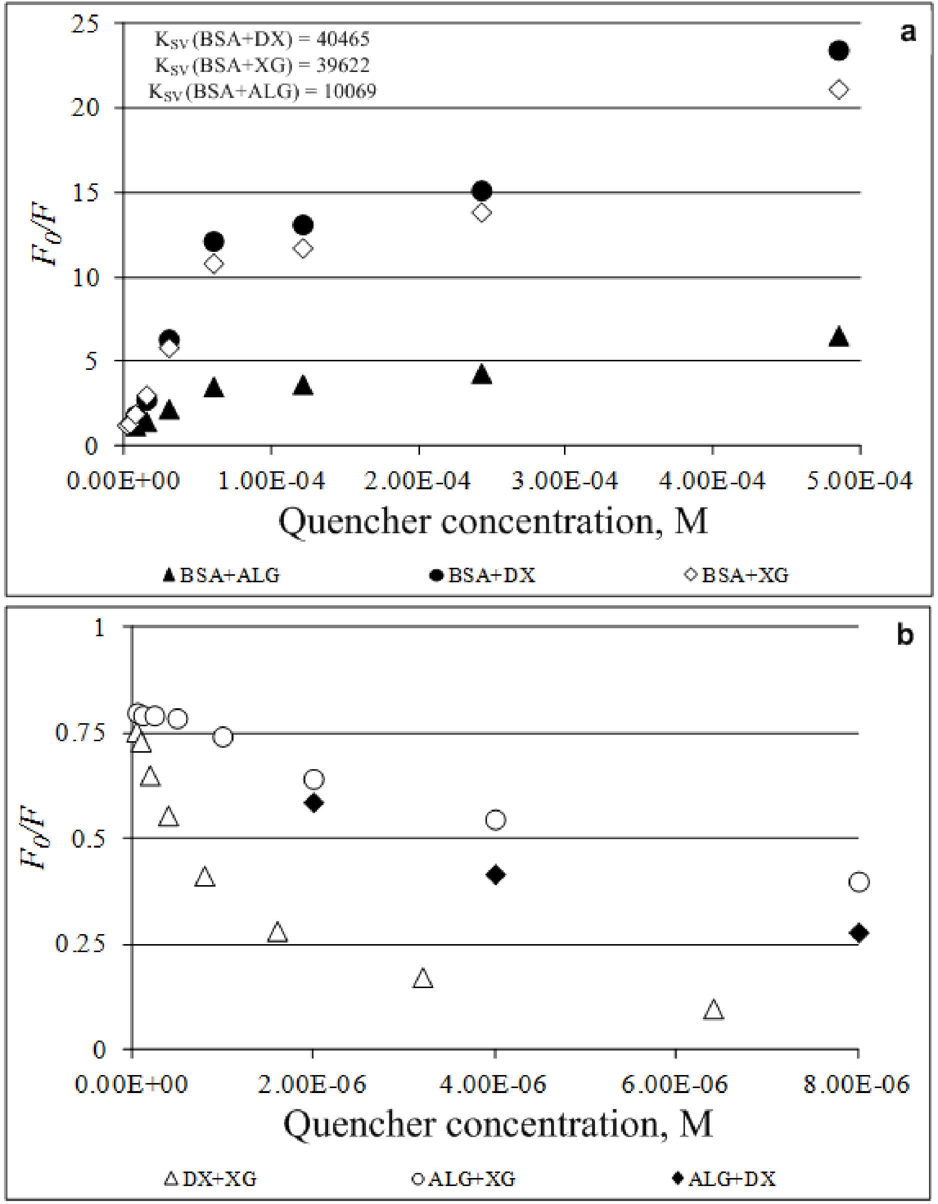

Figure 10. Stern-Volmer quenching plots. Certain fluorophore (BSA for Fig. 10a; DX and ALG for Fig. 10b) concentration was chosen to obtain (a) minimal or (b) maximal detectable fluorescence signal. This is due to the decrease of fluorescence intensity of quenched substances and the increase of fluorescence intensity of unquenched substances. Pre-experiments were carried out to understand the fluorescent behavior of mixtures (i.e. whether fluoresence signal increases or decreases) (data not shown). The concentration of quencher was gradually increased from 12.5 to 32000 ppm. Sodium chloride concentration was adjusted according to fluorophore concentration to maintain the same foulant-NaCl ratio utilized in FO experiments. K_{sv} was calculated as a slope of Stern-Volmer plot.

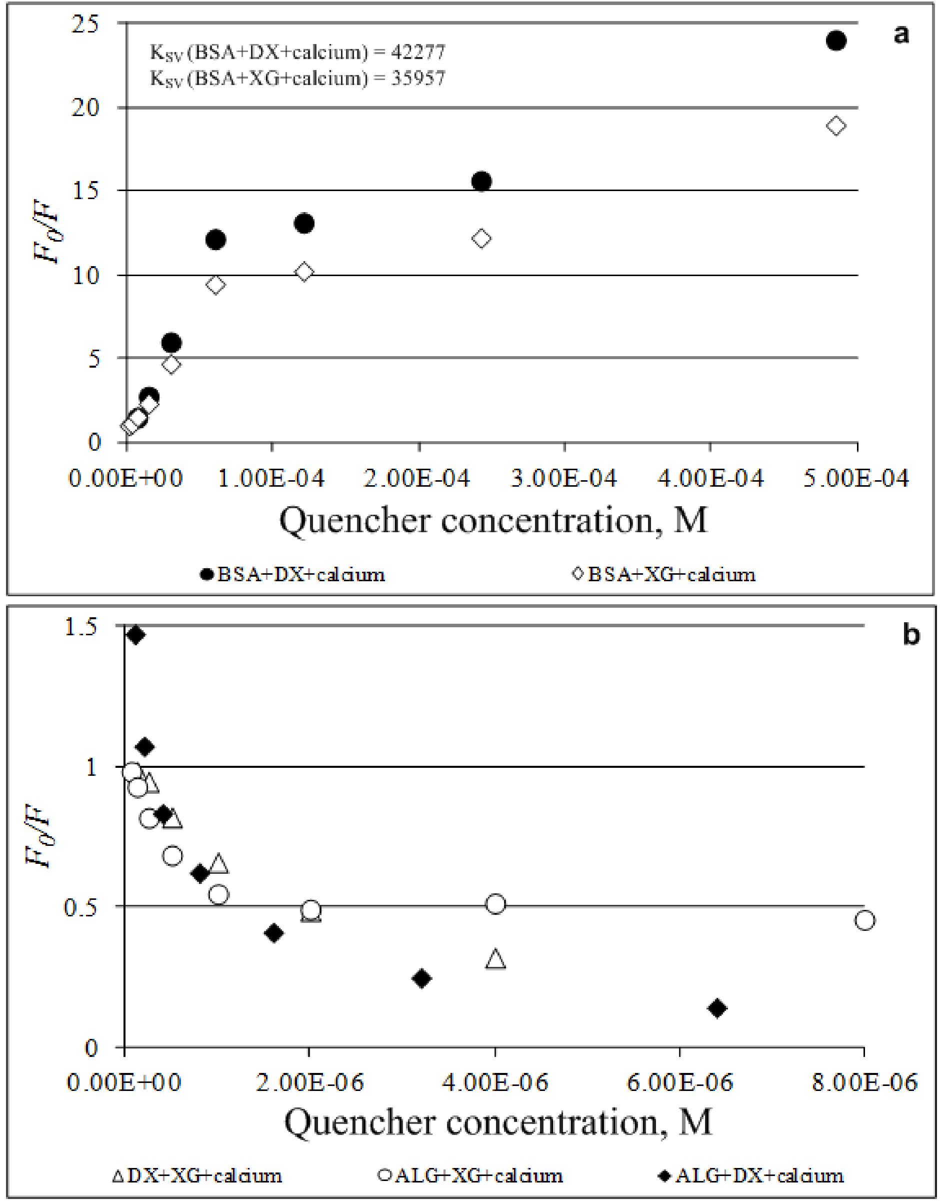

Figure 11. Stern-Volmer quenching plots for solutions containing calcium chloride. Fluorophore (BSA for Fig. 11a; DX and ALG for Fig. 11b) concentration was chosen in the way to obtain (a) minimal or (b) maximal detectable fluorescence signal. It is due to the fact that fluorescence intensity of quenched and unquenched substance decreasing and increasing, respectively. Pre-experiments were carried out to understand fluorescent behavior of mixtures (i.e. whether fluoresence signal increasing or decreasing) (data not shown). Concentration of quencher was gradually increased from 12.5 to 32000 ppm. Sodium and calcium chloride concentrations were adjusted accordingly to fluorophore concentration to maintain same foulant-NaCl-$CaCl_2$ ratio utilized in FO experiments. K_{sv} was calculated as a slope of Stern-Volmer plot.

Table 1. Experimental and theoretical (additive) flux declines.

Foulant	**Flux decline, %**		
	No Ca^{2+}		**With Ca^{2+}**
	Experimental	**Additive**	**Experimental**
BSA	0		0
ALG	0		22
DX	6		0
XG	22		28
BSA+ALG	10	0	36
BSA+DX	1	0	1
BSA+XG	30	22	26
ALG+DX	17	6	23
ALG+XG	18	22	27
DX+XG	36	28	32
BSA+ALG+DX	15	6	25
BSA+ALG+XG	26	22	32
BSA+DX+XG	34	28	33
ALG+DX+XG	36	28	32
ALG+DX+XG+BSA	32	28	39

Table 2. Hydrodynamic diameter and zeta potential of single foulants and selected foulant complexes.

Foulant	Hydrodynamic diameter, nm		Zeta potential, mV	
	No Ca^{2+}	With Ca^{2+}	No Ca^{2+}	With Ca^{2+}
BSA	6	6	-14	-11
ALG	14	45	-44	-30
DX	13	8	-1	-1
XG	54	71	-59	-41
BSA+ALG	6	6	-47 and -32 **	-33
BSA+DX	7	8	-17	-8
BSA+XG	8	9	-58	-37
ALG+DX	16 and 25*	---	-34 and +3**	---
ALG+XG	20	---	- 58	---
DX+XG	16	16	-58	-38

Experimental conditions during hydrodynamic diameter and zeta potential measurements: 66.7 ppm of foulant, 10 mM NaCl, 1 mM $CaCl_2$, pH 6.25-6.5, temperature 23 °C.

*These values indicate the existence of two hydrodynamic diameter peaks.
**These values indicate the existence of two zeta potential peaks.

Table 3. Changes in flux and physico-chemical properties of binary foulants as opposed to the changes obtained with individual foulants without the presence of calcium.

Foulant	Water flux decline	Chemical bonding (EEM)	Viscosity (value in Pa·s)	Size/ Zeta potential
BSA+ALG	✓	+	✓(0.01)	✓
BSA+DX	x	+	✓(0.05)	✓
BSA+XG	✓	+	✓(0.51)	✓
ALG+DX	✓	↔	x(0.01)	✓
ALG+XG	✓	↔	✓(0.53)	✓
DX+XG	✓	↔	✓(0.41)	✓

✓ change in flux/viscosity/zeta potential/size
x no change in flux/viscosity/zeta potential/size
+ foulants establish chemical bonds
↔ foulants do not establish chemical bonds